

High Precision Robust Automatic Alignment Method for Rotating Shaft

J. Luo^{1,2}, Z. Wang^{1*}, C. Shen^{1,2}, S. Liu¹ and Z. Wen^{1,2}

¹Changchun Institute of Optics, Fine Mechanics and Physics, Chinese Academy of Science, Changchun 130033, China

²University of the Chinese Academy of Sciences, Beijing 10049, China

Received: 08 October 2015 / Accepted: 19 June 2016 / Published online: 30 June 2016

© Metrology Society of India 2016

Abstract: Rotating Shaft is widely used in various high precision instruments on scientific and industrial metrology. This paper proposes a high precision and robust method to automatically align a rotating shaft perpendicular to the horizontal plane. Firstly, an alignment model consisting of a dual-axis inclinometer and four motors is designed. Then the rotating shaft tilt angle between the practical and the ideal shaft is projected to two orthogonal planes, and generates a rotation angle in each plane. The two rotation angles are calculated by differential measurement method based on the inclinometer outputs, and then the relationship of shaft tilt angle against inclinometer outputs is obtained. According to these two rotation angles, the relative heights of the three supporting points of the platform attached to the rotating shaft are calculated. Employing an angle closed loop strategy; the rotating shaft tilt angle is aligned by three linear stepping motors. Experiment results show an alignment precision of 0.003° is achieved using an inclinometer with the resolution of 0.0005° and a linear stepping motor with the regulation precision of $0.89 \mu\text{m}$. The proposed method is suitable for a wide variety of precision machines that require the use of rotating shaft.

Keywords: Precision measurement; Inclinometer; Differential measurement; Alignment; Angle closed loop

1. Introduction

Rotating shaft [1] alignment is vital for a large number of precision instruments, such as three-dimensional profile rotary measurement systems [2], rotary-laser based coordinate measurement systems [3], optical level instruments [4] and north-finder [5–7]. Aligning the rotating shaft vertical to the horizontal plane is a prerequisite of achieving high measurement precision. Usually, the rotating shaft is assembled on a center of a platform; ideally, they are perpendicular to each other, but it is not case in practical situations. Placed in different locations, the angle between the platform and the horizontal varies. Due to these above two reasons, the rotating shaft is very likely not to be vertical to the horizontal plane. In order to guarantee that the angle between the practical rotating shaft and the vertical shaft remains in the range of $[0^\circ 0.003^\circ]$, it is essential to measure it and to align the rotating shaft to vertical state.

An ideal rotating shaft alignment method should have high precision, be robust and automatic. It needs to be compatible with different sizes, locations (inside or outside of the instruments) and smoothness of the rotating shaft. Currently, most researches on this topic are focused on platform leveling and multi-shaft alignment. Fang [8] and Liu [9] utilize several inclination sensors to measure the deformation of ultra-precision platform with work pieces on it, and regulate the supporting points based on the inclination sensors' feedback signals. Lu [10] introduces a vehicle-borne radar platform leveling system that provides a leveling precision of 0.017° . However, the sensors in these methods must be pre-calibrated accurately before measurement. Their outputs need to be compensated during the measurement process due to noise disturbances and temperature drifts [11]. Therefore, the precision of the above techniques are seriously affected by the temperature drifts and installation precision of sensors. Multi-shaft alignment is achieved by combining optical devices and micrometer screw measurements [12–15]. For signal rotating shaft alignment, several researchers use different methods to measure the rotating shaft tilt angle, but the problem of aligning the rotating shaft is not solved. Tanachaikhan [16]

*Corresponding author, E-mail: wangzhiqian2000@gmail.com

measures the shaft tilt by recording the magnetic flux density, but it provides a very low shaft tilt angle resolution at 1° . Optical devices are used to measure the deviation angle of various objects [17], however, the rotating shaft must be located outside for light projection. Fan uses two displacement sensors to measure the distances from each sensor to the shaft surface, and the shaft tilt is obtained using their geometric relationships [18]. Fan’s method requires roundness measuring techniques to guarantee that the rotating shaft’s surface is smooth enough [19, 20]; otherwise the result is not accurate.

This paper uses a novel approach to measure the rotating shaft tilt angle and to align it automatically. The rotating shaft tilt is projected to two orthogonal planes, and generates a rotation angle in each plane. From the inclinometer outputs, the two rotation angles are calculated by differential measurement method and the shaft tilt is obtained. The relative heights of three supporting points with respect to the horizontal plane are calculated using coordinate transformations. In order to achieve high alignment precision, two angle closed loop alignment processes are performed. The first quickly aligns the rotating shaft, and the second ensures and further improves the alignment precision. In all, our system achieves high alignment precision regardless of the inclinometer temperature drifts, the size and install location of the rotating shaft.

The rest of the paper is organized as follows. Section 2 presents the overview of the automatic alignment system. Section 3 introduces the rotating shaft tilt measurement method. The proposed rotating shaft alignment algorithm is described in Sect. 4. Section 5 validates the proposed method. Finally, conclusions are drawn in Sect. 6.

2. Automatic Alignment System Overview

The setup of the rotating shaft automatic alignment system is shown in Fig. 1a, and its corresponding mechanical layout is shown in Fig. 1b. It includes two parts; the rotating shaft tilt measuring part (black in Fig. 1b) and the rotating shaft alignment part (red in Fig. 1b). The former part consists of an inclinometer, a platform, a bearing, a torque motor, an encoder and a pedestal. The latter part comprises three screw rods, six limit switches, three plastic sheets, three support legs and three linear stepping motors. The inclinometer is mounted on the platform that is fixed to the rotating shaft. The inclinometer measures the angle between the platform and the horizontal plane. The torque motor rotates the rotating shaft, hence the inclinometer and the platform rotates along with it. The encoder records the rotation angle of the rotating shaft. Six limit switches and three plastic sheets record the highest and lowest position of three linear stepping motors. A, B and C in Fig. 1a are the supporting points of the three supporting legs. Three linear stepping motors control the three screw rods to move A, B and C up and down; hence the tilt angle of the rotating shaft is adjusted.

3. Differential Measurement of the Rotating Shaft

Based on the mechanical layout in Fig. 1b, a shaft tilt measuring model is developed. As shown in Fig. 2, in the Cartesian world coordinate system OXYZ, point O is the geometric center of the inclinometer. OR_0 and OR_1 denote the ideal and practical rotating shafts respectively. The

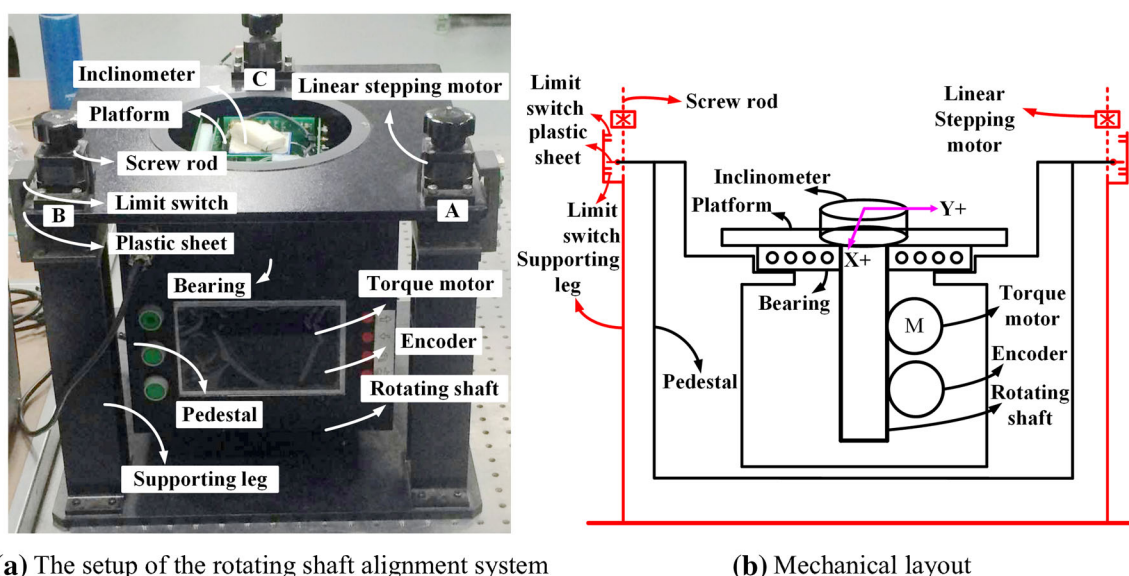


Fig. 1 Rotating shaft automatic alignment setup and its corresponding mechanical layout

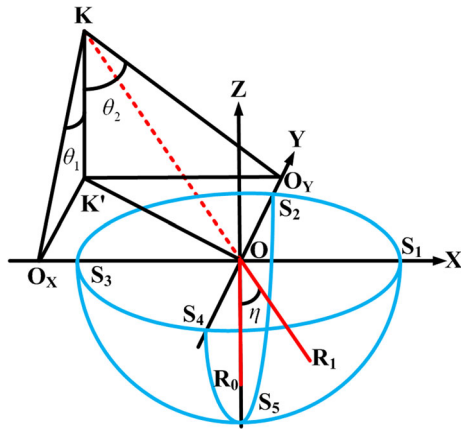


Fig. 2 Rotating shaft tilt measuring model

angle between them, i.e. η , is the rotating shaft tilt angle. The practical rotating shaft OR_1 may locate in four areas, i.e. $OS_1S_2S_5$, $OS_2S_3S_5$, $OS_3S_4S_5$ and $OS_4S_1S_5$. Figure 2 shows the case when OR_1 is in the $OS_4S_1S_5$ area. OK is the extension line of OR_1 . KK' is parallel to axis Z ; $K'O_X$ and O_Y are parallel to axis Y and X respectively. Therefore the O_YKK' plane is parallel to the O_XZ plane and the O_XKK' plane is parallel to the OYZ plane. θ_1 is the angle between KK' and KO_X , and θ_2 is that between KK' and KO_Y . According to geometric relationships, the shaft tilt angle η is obtained,

$$\eta = \arctan \sqrt{(\tan \theta_1)^2 + (\tan \theta_2)^2}. \tag{1}$$

In order to calculate η , θ_1 and θ_2 should be obtained first. In Fig. 2, OR_1 is obtained by rotating OR_0 twice consecutively, once about axis X and the other about axis Y . Using the right hand rules, the first rotation is rotating counterclockwise through an angle $-\theta_1$ about the X axis. The second one is rotating clockwise through an angle $-\theta_2$ about the Y axis; here $\tan(O_XKO)/\cos \theta_1 = \tan \theta_2$,

usually θ_1 is less than 1° , hence $\theta_2 \approx O_XKO$. Therefore, in the following calculation, θ_2 is used to denote angle O_XKO .

As shown in Fig. 3a, when the practical rotating shaft coincides with the ideal one ($\eta = 0$), OX_0 , OY_0 and OR_0 indicate the inclinometer axis $X+$, axis $Y+$ and the rotating shaft respectively. OX_0 , OY_0 and OR_0 are defined as unit vectors, and here $OX_0 = (0, -1, 0)^T$; $OY_0 = (1, 0, 0)^T$; $OR_0 = (0, 0, -1)^T$. The rotating shaft has two properties. Firstly, when the rotating shaft is vertical, i.e. $\eta = 0$, the inclinometer outputs of $X+$ and $Y+$ axes remain the same regardless of the shaft's rotation about itself. Secondly, the tilt angle between the practical shaft and ideal one is fixed no matter how the shaft rotates about itself. OR_1 in Fig. 3b is obtained by rotating OR_0 in Fig. 3a about X axis (counterclockwise through an angle θ_1) and Y axis (clockwise through an angle θ_2) consecutively; meanwhile OX_0 and OY_0 transform into OX_1 and OY_1 respectively. Using the right hand rules, the rotation matrixes are,

$$\mathbf{Rot}(X, \theta_1) = \begin{bmatrix} 1 & 0 & 0 \\ 0 & \cos \theta_1 & -\sin \theta_1 \\ 0 & \sin \theta_1 & \cos \theta_1 \end{bmatrix} \tag{2}$$

$$\mathbf{Rot}(Y, \theta_2) = \begin{bmatrix} \cos \theta_2 & 0 & \sin \theta_2 \\ 0 & 1 & 0 \\ -\sin \theta_2 & 0 & \cos \theta_2 \end{bmatrix} \tag{3}$$

Therefore, vector OX_1 , OY_1 and OR_1 are achieved,

$$\begin{cases} OX_1 = \mathbf{Rot}(Y, \theta_2) \mathbf{Rot}(X, \theta_1) OX_0 \\ OY_1 = \mathbf{Rot}(Y, \theta_2) \mathbf{Rot}(X, \theta_1) OY_0 \\ OR_1 = \mathbf{Rot}(Y, \theta_2) \mathbf{Rot}(X, \theta_1) OR_0 \end{cases} \tag{4}$$

Substituting (2) and (3) into (4), and we have:

$$\begin{cases} OX_1 = (-\sin \theta_1 \sin \theta_2, -\cos \theta_1, -\sin \theta_1 \cos \theta_2)^T \\ OY_1 = (\cos \theta_2, 0, -\sin \theta_2)^T \\ OR_1 = (-\cos \theta_1 \sin \theta_2, \sin \theta_1, -\cos \theta_1 \cos \theta_2)^T \end{cases} \tag{5}$$

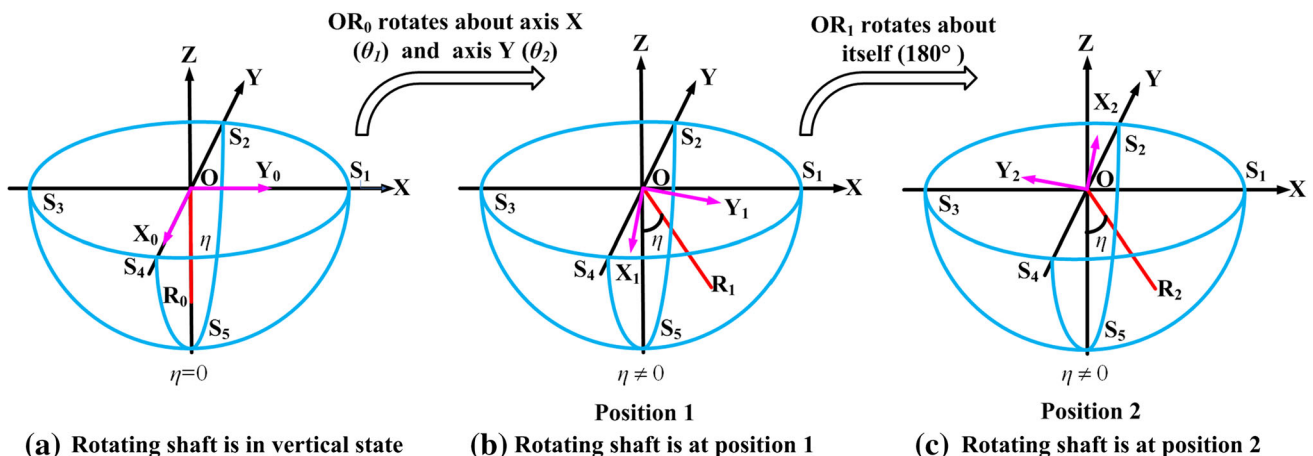


Fig. 3 Rotating shaft tilt measurement process

Rotating OR_1 in Fig. 3b counterclockwise through 180° about itself, Fig. 3c is obtained. After the rotation, OX_1 and OY_1 change to $OX_2 = (xx_2, yy_2, zz_2)$ and $OY_2 = (xy_2, yy_2, zy_2)$ respectively. OX_2 is a unit vector; OX_2 is perpendicular to OR_1 ; the angle of vector OX_2 against vector OX_1 is 180° . Based on these conditions, a set of equations about vector OX_2 is obtained:

$$\begin{cases} xx_2^2 + yy_2^2 + zz_2^2 = 1 \\ -\cos \theta_1 \sin \theta_2 xx_2 + \sin \theta_1 yy_2 - \cos \theta_1 \cos \theta_2 zz_2 = 0 \\ -\sin \theta_1 \sin \theta_2 xx_2 - \cos \theta_1 yy_2 - \sin \theta_1 \cos \theta_2 zz_2 = -1 \end{cases} \quad (6)$$

Similarly, a set of equations about vector OY_2 are achieved:

$$\begin{cases} xy_2^2 + yy_2^2 + zy_2^2 = 1 \\ -\cos \theta_1 \sin \theta_2 xy_2 + \sin \theta_1 yy_2 - \cos \theta_1 \cos \theta_2 zy_2 = 0 \\ \cos \theta_2 xy_2 - \sin \theta_2 zy_2 = -1 \end{cases} \quad (7)$$

Solving (6) and (7), vector OX_2 and OY_2 are,

$$\begin{cases} OX_2 = (\sin \theta_1 \sin \theta_2, \cos \theta_1, \sin \theta_1 \cos \theta_2)^T \\ OY_2 = (\cos \theta_2, 0, \sin \theta_2)^T \end{cases} \quad (8)$$

The inclinometer outputs of the $X+$ and $Y+$ axes at position 1 are θ_{x1} and θ_{y1} respectively, and those at position 2 are θ_{x2} and θ_{y2} respectively. Based on (5), (8) and the inherent property of the inclinometer, we have:

$$\begin{cases} \sin(\theta_{x1}) = -\sin \theta_1 \cos \theta_2 \\ \sin(\theta_{x2}) = \sin \theta_1 \cos \theta_2 \end{cases} \quad (9)$$

$$\begin{cases} \sin(\theta_{y1}) = -\sin \theta_2 \\ \sin(\theta_{y2}) = \sin \theta_2 \end{cases} \quad (10)$$

Based on (9) and (10), we have,

$$\begin{cases} \sin \theta_1 = (\sin(\theta_{x2}) - \sin(\theta_{x1})) / (2 \cos \theta_2) \\ \theta_2 = (\theta_{y2} - \theta_{y1}) / 2 \end{cases} \quad (11)$$

Generally, θ_1 and θ_2 are small (less than 1°), thus (11) is simplified as,

$$\begin{cases} \theta_1 \approx (\theta_{x2} - \theta_{x1}) / 2 \\ \theta_2 = (\theta_{y2} - \theta_{y1}) / 2 \end{cases} \quad (12)$$

Substituting (12) into (1), the relationship of η against inclinometer outputs is,

$$\eta \approx \arctan \sqrt{\left(\tan \frac{\theta_{x2} - \theta_{x1}}{2}\right)^2 + \left(\tan \frac{\theta_{y2} - \theta_{y1}}{2}\right)^2} \quad (13)$$

As seen from (13), the inclinometer temperature drifts are largely reduced by subtracting the inclinometer outputs at position 1 from the inclinometer outputs at position 2. Additionally, the inclinometer systematic error is eliminated; η is accurate even if the inclinometer is not well-calibrated. Therefore, the measurement method is self-robust and ensures high precision.

4. Align the Rotating Shaft

In order to align the rotating shaft automatically, three supporting points' heights with respect to the horizontal plane are calculated first. Then two angle closed loop alignment processes are performed to decrease the alignment errors contributed by the inclinometer temperature drifts and the missed steps of the linear stepping motor.

4.1. Calculate Three Support Points' Relative Heights

As shown in Fig. 1a, A , B and C denote the supporting points of the three supporting legs. A_0 , B_0 and C_0 denote A , B and C when the shaft is in ideal state ($\eta = 0$) and $A_0B_0C_0$ is parallel to the horizontal plane. In the alignment system, three supporting legs build an isosceles triangle, the side $A_0B_0 = L_1$, the sides $A_0C_0 = B_0C_0 = L_2$. D_0 is the midpoint of A_0B_0 , and O is the midpoint of C_0D_0 . In $OXYZ$, the coordinate of point A_0 , B_0 and C_0 are,

$$\begin{cases} A_0 = \left(\frac{L_1}{2}, -\frac{\sqrt{L_2^2 - (L_1/2)^2}}{2}, 0\right)^T \\ B_0 = \left(-\frac{L_1}{2}, -\frac{\sqrt{L_2^2 - (L_1/2)^2}}{2}, 0\right)^T \\ C_0 = \left(0, \frac{\sqrt{L_2^2 - (L_1/2)^2}}{2}, 0\right)^T \end{cases}$$

The supporting points in horizontal plane are A_0 , B_0 and C_0 when $\eta = 0$. A_1 , B_1 and C_1 denote the practical supporting points when $\eta \neq 0$. A_1 , B_1 and C_1 are achieved by rotating OR_0 twice consecutively from A_0 , B_0 and C_0 respectively, one counterclockwise through an angle θ_1 about the X axis, and the other clockwise through an angle θ_2 about the Y axis. Matrix $\mathbf{Rot}(X, \theta_1)$ and $\mathbf{Rot}(Y, \theta_2)$ represent the first and the second rotation respectively. A_1 , B_1 and C_1 can be expressed as,

$$\begin{cases} A_1 = \mathbf{Rot}(Y, \theta_2) \mathbf{Rot}(X, \theta_1) A_0 \\ B_1 = \mathbf{Rot}(Y, \theta_2) \mathbf{Rot}(X, \theta_1) B_0 \\ C_1 = \mathbf{Rot}(Y, \theta_2) \mathbf{Rot}(X, \theta_1) C_0 \end{cases} \quad (14)$$

The relative heights of points A_1 , B_1 and C_1 are denoted as H_{A1} , H_{B1} and H_{C1} . Substituting (2) and (3) into (14), the following equations are obtained:

$$\begin{cases} H_{A1} = A_1(3, 1) = -\frac{L_1}{2} \sin \theta_2 - \frac{\sqrt{L_2^2 - (L_1/2)^2}}{2} \sin \theta_1 \cos \theta_2 \\ H_{B1} = B_1(3, 1) = \frac{L_1}{2} \sin \theta_2 - \frac{\sqrt{L_2^2 - (L_1/2)^2}}{2} \sin \theta_1 \cos \theta_2 \\ H_{C1} = C_1(3, 1) = \frac{\sqrt{L_2^2 - (L_1/2)^2}}{2} \sin \theta_1 \cos \theta_2 \end{cases} \quad (15)$$

4.2. Angle Closed Loop Regulation Strategy

Aiming at reducing the system complexity and cost, the system does not utilize an encoder for recording the

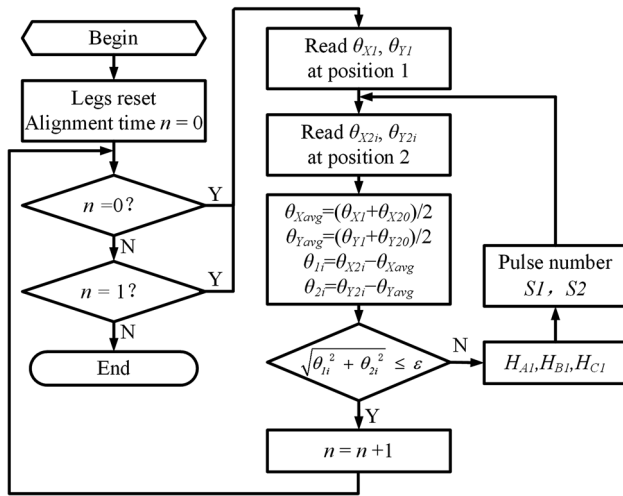


Fig. 4 Overall alignment process

position of the linear stepping motors. Therefore, an angle closed loop regulation strategy is used to eliminate the linear stepping motors’ missed steps and external disturbances. Two alignment steps are performed. The first one quickly aligns the rotating shaft, and the second one examines and further improves the first alignment. The overall alignment process is shown in Fig. 4.

Initially, legs are reset and the number of executed alignment times n is assigned as 0. If n equals 0, the first alignment process begins.

Firstly, the shaft is rotated to position 1, and the inclinometer outputs θ_{X1}, θ_{Y1} are recorded.

Secondly, the shaft is rotated from position 1 to position 2, and inclinometer outputs $\theta_{X2i}, \theta_{Y2i}$ are read, where i denotes the number of iteration during each alignment process. In the first iteration, $i = 1$. The average value of the inclinometer outputs at position 1 and position 2 are hence calculated using the following formula:

$$\begin{cases} \theta_{Xavg} = \frac{\theta_{X2i} + \theta_{X1}}{2} \\ \theta_{Yavg} = \frac{\theta_{Y2i} + \theta_{Y1}}{2} \end{cases} \quad (16)$$

From $\theta_{X2i}, \theta_{Y2i}, \theta_{Xavg}$ and θ_{Yavg} , the i -th iteration angles θ_{1i} and θ_{2i} are obtained:

$$\begin{cases} \theta_{1i} = \theta_{X2i} - \theta_{Xavg} \\ \theta_{2i} = \theta_{Y2i} - \theta_{Yavg} \end{cases} \quad (17)$$

In the first iteration, i.e. $i = 1$, the first iteration angles are obtained by substituting (16) into (17),

$$\begin{cases} \theta_{11} = \frac{\theta_{X21} - \theta_{X1}}{2} \\ \theta_{21} = \frac{\theta_{Y21} - \theta_{Y1}}{2} \end{cases} \quad (18)$$

Clearly, (18) coincides with (12).

Thirdly, the shaft tilt is calculated based on (13). It is then compared with a threshold ϵ . If η is less than ϵ , n adds

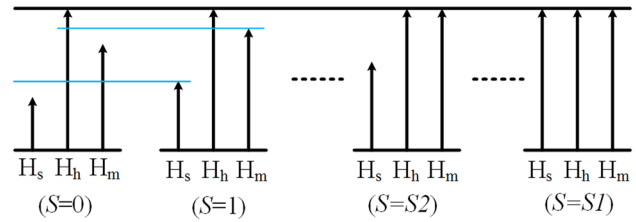


Fig. 5 Highest leg unmoved regulation strategy in each iteration

1 on itself; otherwise the relative height of three supporting points H_{A1}, H_{B1}, H_{C1} are calculated based on (15). In order to reduce the alignment time, three legs are at the low limit switches before regulation. As shown in Fig. 5, in each iteration process, the highest leg remains unmoved, and the other two lower legs are risen up simultaneously to acquire better dynamic performance. Therefore the pulse numbers of two linear stepping motors (corresponding to the two lower legs) are,

$$\begin{cases} S1 = \frac{H_h - H_s}{\rho} \\ S2 = \frac{H_h - H_m}{\rho} \end{cases} \quad (19)$$

where ρ denotes the linear stepping motor’s minimum step; H_h, H_m, H_s denote the largest, middle, smallest number of H_{A1}, H_{B1}, H_{C1} respectively. As shown in Fig. 5, using S to denote the pulse number. In each iteration process, the lowest leg and the middle leg move one step from $S = 0$ to $S = 1$; the middle leg stops when $S = S2$; the lowest keeps moving until S reaches $S1$. Due to the linear stepping motors’ missed steps and external disturbances, it is difficult to achieve the end condition ($\eta \leq \epsilon$) by executing only one iteration. Usually, more than one iteration are executed until the end condition is met. The second alignment is executed if the first one ends and $n = 1$ is detected. The same alignment steps as the first alignment are followed.

5. Experiment

A platform based on the mechanical layout in Fig. 1 is built to test the proposed alignment method. The inclinometer’s respond time is 0.3 s. Its zero temperature drift is less than $5 \times 10^{-4}/^\circ\text{C}$ and its sensitivity is smaller than $1 \times 10^{-3}/^\circ\text{C}$. Therefore the inclinometer outputs remain stable in a short period of time, and shall fluctuate heavily if the inclinometer is being used for a long time. Three identical linear stepping motors are selected to rise up and drop down the three screw rods. The minimum step of the linear stepping motor is $1.98 \mu\text{m}$. Driving by a DCM4010 driver, it can reach $0.03 \mu\text{m}$. Six infrared sensors are used as limit switches. When the supporting point reaches the highest or the lowest position, the infrared light is shielded by the

plastic sheet hence the output voltages of the infrared sensors jump to high level from low level. PID algorithm is adapted to control the torque motor to ensure fast rotation speed of the rotating shaft. The whole system is controlled by a C8051F020 micro-control unit. Three groups of experiments are conducted to verify the proposed method, as shown in Sects. 5.1, 5.2 and 5.3.

5.1. Rotating Shaft Tilt Measurement

The rotating shaft tilt is measured before the alignment process. The experiment device was placed on a steady platform. Initially, the inclinometer and the rotating shaft is moved to position 1 by the torque motor and the inclinometer outputs θ_{X1} , θ_{Y1} are recorded; afterwards the inclinometer and the shaft is rotated 180° to position 2 and the inclinometer outputs θ_{X2} , θ_{Y2} are recorded. In every 5 min, such procedures are conducted once again. The entire experiment lasts 165 min.

Figure 6 shows the values of θ_1 , θ_2 and η , which are calculated based on θ_{X1} , θ_{Y1} , θ_{X2} and θ_{Y2} . Over the 165 min, the range of θ_1 , θ_2 and η are 0.005°, 0.004° and 0.0025° respectively, and the standard deviation of θ_1 , θ_2 and η are 0.0012°, 0.0009° and 0.0007° respectively. In conclusion, θ_1 , θ_2 and η are stable over a long period of time and the measurement method is effective.

5.2. Automatic Alignment

The measurement and regulation precision affect the shaft alignment precision. A proper linear stepping motor’s minimum step ρ is chosen to guarantee that the regulation precision is higher than the measurement precision. According to the error estimation theory, we have:

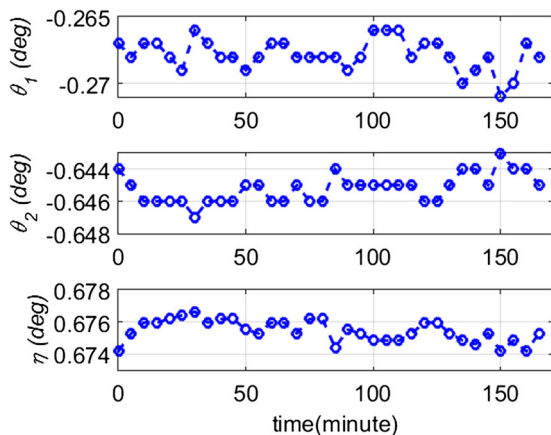


Fig. 6 The rotating shaft tilt measurement

$$\begin{cases} \sigma_1 = \sqrt{\left(\frac{\partial \eta}{\partial \theta_{X1}}\right)^2 d\theta^2 + \left(\frac{\partial \eta}{\partial \theta_{Y1}}\right)^2 d\theta^2}, & i = 1, 2 \\ \sigma_2 = \sqrt{\left(\frac{\partial \eta}{\partial H_{A1}}\right)^2 \rho^2 + \left(\frac{\partial \eta}{\partial H_{B1}}\right)^2 \rho^2 + \left(\frac{\partial \eta}{\partial H_{C1}}\right)^2 \rho^2}, \\ \sigma_3 = \sqrt{\sigma_1^2 + \sigma_2^2} \end{cases} \quad (20)$$

where $d\theta$ denotes the inclinometer resolution, ρ denotes the minimum step of each linear stepping motor, σ_1 , σ_2 , σ_3 denote the shaft measurement precision, the rotating shaft tilt regulation precision and the overall alignment precision respectively. In our system, the rotating shaft tilt measurement precision σ_1 is 0.0007°. The regulation precision σ_2 is 0.0006° when the linear stepping motor’s minimum step ρ is set at 0.99 μm . Hence the overall alignment precision σ_3 is approximately 0.001°. The threshold ε is set at 0.002°. As shown in Fig. 2, the rotating shaft can be located in four sections. Using the right hand rules, $\theta_1 > 0$ ($\theta_1 < 0$) when OR is rotated counterclockwise (clockwise) through an angle θ_1 about X axis; $\theta_2 > 0$ ($\theta_2 < 0$) when OR is rotated clockwise (counterclockwise) through an angle θ_2 about Y axis. Therefore, the rotating shaft has four cases according to the sign of θ_1 and θ_2 . They are $\theta_1 > 0$ and $\theta_2 > 0$; $\theta_1 > 0$ and $\theta_2 < 0$; $\theta_1 < 0$ and $\theta_2 > 0$; $\theta_1 < 0$ and $\theta_2 < 0$.

To align the rotating shaft, the proposed angle close loop strategy described in Sect. 4.2 is used. Figure 7 shows the rotating shaft tilt alignment process in four cases. Before regulation, 1 s is taken for recording inclinometer outputs at position 1; 3 s are taken for rotating shaft from position 1 to position 2 and another 1 s for recording inclinometer outputs at position 2; hence 5 s are taken in total. In each iteration process, the outputs of the inclinometer $X+$ and $Y+$ axes are simultaneously measured after S reaches $S1$. The initial shaft tilt angles are 0.5229°, 0.2866°, 0.3216° and 0.409° in Fig. 7a–d respectively. Their shaft tilt angles reduce to 0.0014°, 0.001°, 0.0014° and 0.0014° after the first alignment which includes three iterations. Then it takes 8 s to start the second alignment, 3 s to rotate the shaft from position 2 back to position 1, and another 5 s to make preparations for the second alignment as the first one. At the beginning of the second alignment, the shaft tilt angles in four cases are 0.0028°, 0.005°, 0.0028° and 0.0028° which are bigger than 0.002°. After 2 iterations in second alignment, the shaft tit angles reach 0.001°, 0.0014°, 0.001 and 0.0014°.

5.3. Analysis of the Rotating Shaft Alignment

An electronic level meter with accuracy of 0.0006° is utilized to analyze the alignment results in four cases. The electronic level meter is placed on the top of the inclinometer, as shown in Fig. 8a. After the alignment process in Fig. 7, the torque motor controls the shaft, the platform,

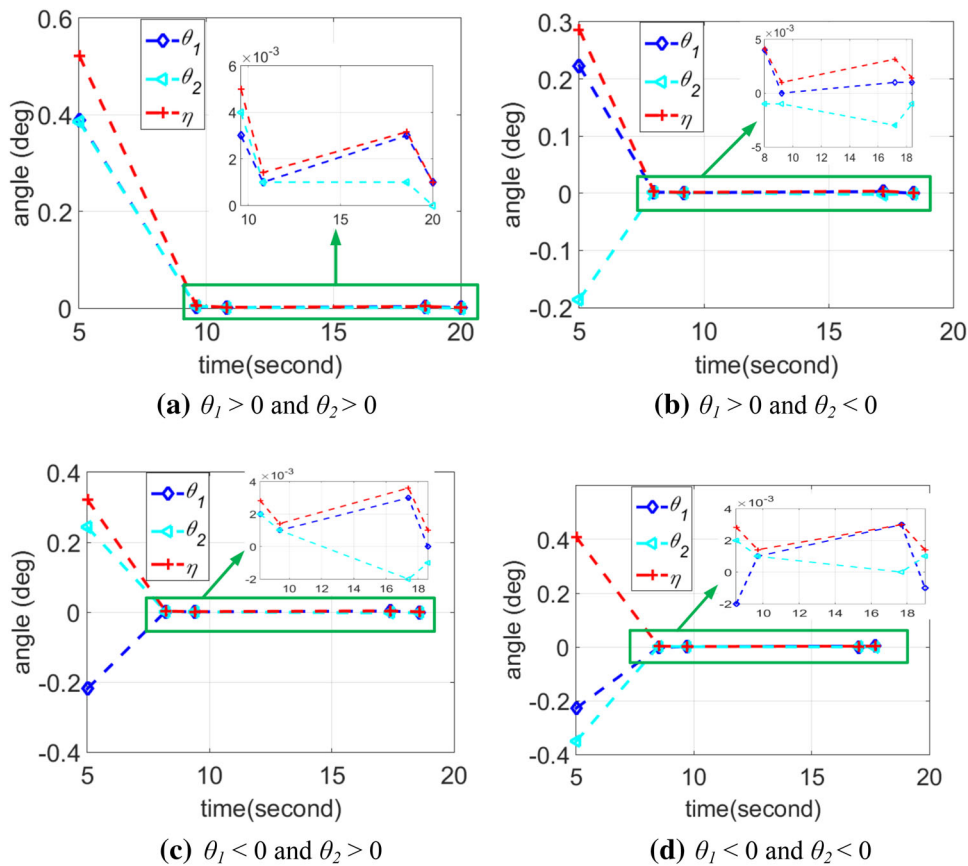


Fig. 7 Rotating shaft automatic alignment process in four cases

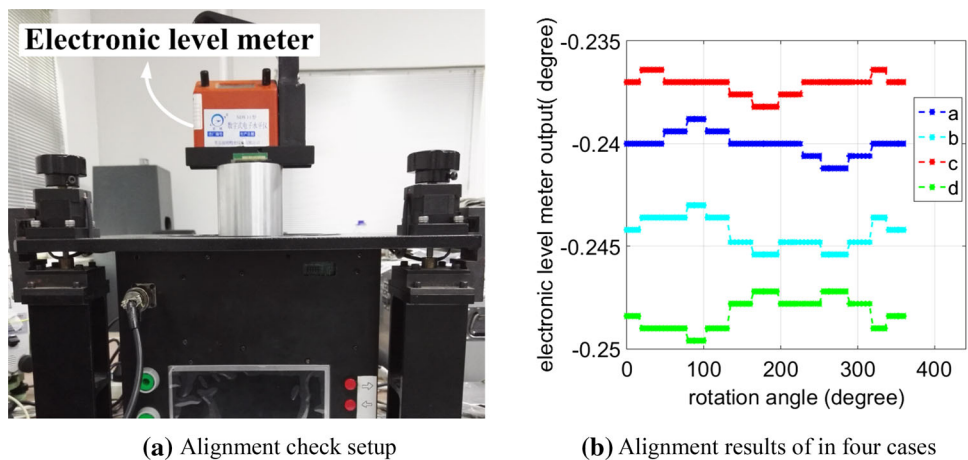


Fig. 8 Analysis of the alignment results

the inclinometer and the electronic level meter to consecutively rotate in one direction for 72 times, each time for 5°, thus 360° in total. At each of the 72 positions, the angles between the electronic level meter surface and the horizontal plane are recorded by the electronic level meter.

Figure 8b shows the data recorded by the electronic level meter. The rotating shaft tilt angles in four cases are 0.0024°, 0.0027°, 0.0012° and 0.0027° respectively. The ranges of electronic level meter outputs in four cases are 0.0024°, 0.0024°, 0.0018° and 0.0024° respectively.

6. Conclusion

This paper proposes a high precision robust method to automatically align rotating shaft. Firstly, it measures the rotating shaft tilt using a dual axis inclinometer. The zero temperature drifts of the inclinometer are effectively decreased by the proposed measuring model and differential measurement method. Therefore, high precision tilt measurement results are obtained. Secondly, three linear stepping motors are used to regulate the rotating shaft tilt. Coordinate transformation is used to calculate three supporting points' relative heights. Two angle closed loop alignment procedures are performed to overcome the linear stepping motors' missed steps and external disturbances. Each alignment process guarantees the rotating shaft tilt to be smaller than a predetermined threshold. The first alignment quickly reduces the angle of the rotating shaft tilt to a fairly small value; the second one ensures and further improves the regulation precision. Finally, the alignment result is validated by an electronic level meter with a higher precision than the threshold.

It is possible to manually align the rotating shaft. In such a condition, it should be guaranteed that the outputs of the inclinometer at position 1 equals those at position 2. However, this method expenses a large amount of alignment time.

The proposed method is robust and accurate, and meets the requirement of most precision machines that require the use of rotating shaft. Higher precision and faster alignment speed shall be achieved with the use of an inclinometer that has a higher resolution and a faster sampling speed. We plan to further this work by combing the vertical rotating shaft and a gyroscope to measure azimuth.

Acknowledgments The work is supported by the Jilin Province key scientific and technological projects of China (20150204013GX).

References

- [1] Luo J, Wang Z, Shen C, et al. Rotating shaft tilt angle measurement using an inclinometer. *Measurement Science Review*, 2015, 15(5): 236–243.
- [2] Chen B, Zhang X, Zhang H, et al. Investigation of error separation for three dimensional profile rotary measuring system. *Measurement*, 2014, 47: 627–632.
- [3] Liu Z, Zhu J, Yang L, et al. A single-station multi-tasking 3D coordinate measurement method for large-scale metrology based on rotary-laser scanning. *Measurement Science and Technology*, 2013, 24(10): 105004.
- [4] Sidki H M. New Test Method for Surveying Optical Level Instruments Using CMM as a Distance Comparator Technique. *MAPAN - Journal of Metrology Society of India*, 2015, 30(2): 139–144.
- [5] Prikhodko I P, Zotov S, Trusov A, et al. What is MEMS gyro-compassing? Comparative analysis of maytagging and carouseling. *Microelectromechanical Systems, Journal of*, 2013, 22(6): 1257–1266.
- [6] Mu-Jun X, Li-Ting L, Zhi-Qian W. Study and application of variable period sampling in strap-down north seeking system. *Energy Procedia*, 2012, 16: 2081–2086.
- [7] Arnaudov R, Angelov Y. Earth rotation measurement with micromechanical yaw-rate gyro. *Measurement Science and Technology*, 2005, 16(11): 2300.
- [8] Liu Y, Fang S, Otsubo H, et al. Simulation and research on the automatic leveling of a precision stage. *Computer-Aided Design*, 2013, 45(3): 717–722.
- [9] Fang S, Liu Y, Otsubo H, et al. An automatic leveling method for the stage of precision machining center. *The International Journal of Advanced Manufacturing Technology*, 2012, 61(1–4): 303–309.
- [10] Lu C, Huang D, Jin Z, et al. The Research and Design of Auto-leveling Control System for Vehicle-borne Radar Platform Based on AVR, Mechatronic and Embedded Systems and Applications, *Proceedings of the 2nd IEEE/ASME International Conference on*. IEEE, 2006: 1–5.
- [11] Shang Z, Ma X, Li M, et al. High-Precision Calibration for MEMS Gyroscopes Based on Persistent Excitation Signal Criterion. *MAPAN - Journal of Metrology Society of India*, 2015, 30(3): 161–168.
- [12] Liao T T. Modeling and analysis of laser shaft alignment using 4×4 homogeneous coordinate transformation matrix. *Measurement*, 2009, 42(1): 157–163.
- [13] Jiao G, Li Y, Zhang D, et al. A laser shaft alignment system with dual PSDs. *Journal of Zhejiang University SCIENCE A*, 2006, 7(10): 1772–1776.
- [14] Hemming B. Calibration of shaft alignment instruments, *SPIE's International Symposium on Optical Science, Engineering, and Instrumentation*. International Society for Optics and Photonics, 1998: 290–297.
- [15] Khaled K M, Aggag G, Abuelezz A E, et al. The influence of misalignment on the uncertainty of vertical torque calibration machine. *MAPAN - Journal of Metrology Society of India*, 2011, 26(2): 153–157.
- [16] Tanachaikhan L, Tammarugwattana N, Sriratana W, et al. Declined angle analysis of shaft using magnetic field measurement, *ICCAS-SICE*, 2009. IEEE, 2009: 1846–1849.
- [17] Luo J, Zhao W. Autocollimator for Small Angle Measurement over Long Distance, *Proceedings of the 27th Conference of Spacecraft TT&C Technology in China*. Springer Berlin Heidelberg, 2015: 263–271.
- [18] Fan K C, Liang M W. Development of an automatic cumulative-lead error measurement system for ballscrew nuts. *The International Journal of Advanced Manufacturing Technology*, 2014, 72(1–4): 17–23.
- [19] Lei X Q, Pan W M, Tu X P, et al. Minimum Zone Evaluation for Roundness Error Based on Geometric Approximating Searching Algorithm. *MAPAN - Journal of Metrology Society of India*, 2014, 29(2): 143–149.
- [20] Sridharan K, Sivaramakrishnan R. Compression and Deformation of Cylindrical Rubber Blocks. *MAPAN - Journal of Metrology Society of India*, 2014, 29(2): 107–114.